Proc. Natl. Acad. Sci. USA
Vol. 79, pp. 6712–6716, November 1982
Neurobiology

Discrete changes of cell membrane capacitance observed under conditions of enhanced secretion in bovine adrenal chromaffin cells

(exocytosis/endocytosis/patch clamp/release)

E. NEHER AND A. MARTY*

Max-Planck-Institut für Biophysikalische Chemie, Am Fassberg, D-3400 Göttingen, Federal Republic of Germany

Communicated by S. Hagiwara, July 2, 1982

ABSTRACT **The capacitance of the surface membrane of small adrenal chromaffin cells was measured with patch-clamp pipettes. Continuous and discrete changes of capacitance were observed. They were interpreted as changes of surface area connected to exocytotic or endocytotic processes. Most of the measurements were performed in the "whole-cell" recording configuration [Hamill, O. P., Marty, A., Neher, E., Sakmann, B. & Sigworth, F. J. (1981) *Pflügers Arch.* 391, 85–100], which allows the intracellular Ca^{2+} concentration to be controlled. With an internal solution highly buffered to low values of Ca^{2+} concentration (10 nM), the surface capacitance usually decreased and could not be markedly changed by electrical stimulation. At low buffering capacity and medium Ca^{2+} concentrations (0.1–1 μM), the capacitance measurement showed large fluctuations and discrete steps, reflecting both capacitance decrease and increase. A large transient increase of capacitance could be induced by electrical stimulation under these conditions. It was linked to Ca^{2+} currents through the membrane. Relatively large ($2–6 \times 10^{-14}$ F) steps of capacitance decrease were common after extensive stimulation. The size distribution of step-like capacitance changes is well compatible with the idea that steps of capacitance increase reflect individual events of exocytosis of chromaffin granules, whereas steps of the opposite polarity reflect the formation of vesicles or vacuoles by endocytosis.**

Exocytosis is used by many cell types to transfer vesicle-contained substances such as neurotransmitters (1), hormones (2), or enzymes (3) into the extracellular medium. A comparatively well-studied example of this process is the secretion of catecholamines in chromaffin cells of the adrenal medulla, where Ca^{2+} entry triggers a cycle involving exocytosis of chromaffin granules (4–6), followed by retrieval of membrane from the surface into intracellular vesicles and vacuoles (5–8). Fusion of chromaffin granules with the plasma membrane leads to a transient increase of membrane surface area, soon followed by a surface decrease corresponding to endocytosis. Such changes should be reflected by alterations of the cell membrane capacitance after stimulation. The patch-clamp method constitutes a very sensitive way of measuring membrane currents (9), which, with appropriate voltage command signals, can be used to measure membrane capacitance at high resolution. Here, we show that a sensitivity can be reached that should be sufficient to resolve changes in capacitance expected during exocytosis/endocytosis of single vesicles. Furthermore, we report the observation of discrete changes in the range of 0.4–80 fF (1 fF = 10^{-15} F) that have many of the properties expected for such events.

METHODS

A simple way of measuring the capacitance of a cell membrane is to apply, under voltage-clamp conditions, a sine wave to the membrane and to measure current. At high enough frequencies, the resulting sinusoidal current is roughly proportional to membrane capacitance C, apart from errors introduced by a parallel conductance G (the membrane conductance) and a series conductance G_s (pipette and electrolyte conductance). Both errors can be dealt with in various ways by standard methods of circuit analysis. We chose to use a phase-sensitive detector (or "lock-in amplifier") for this purpose as shown in Fig. 1.

The lock-in amplifier supplies a sine wave (the reference signal), which is used as a command signal to the voltage clamp and accepts the resulting current sine wave as an input. The amplifier can be set to a certain phase angle and then determines that component of the input signal which bears the selected phase relationship to the reference signal. For a simple parallel combination of R and C, the resistive current would be in phase with the command signal and the capacitive current would be phase-shifted by 90° with respect to the reference signal. Thus, in this simple case, setting the phase to 90° would result in an output signal proportional to capacitance and independent of the cell conductance. In our system, an additional phase shift is introduced by the series conductance G_s. Thus, the phase angle appropriate for capacitance measurements is different from 90° and has to be determined on each cell individually as follows.

The admittance of the equivalent circuit of Fig. 1*B* (neglecting the shunt capacitance, C_{sh}) can be expressed in complex notation as

$$Y(\omega) = \frac{G + j\omega C}{1 + G/G_s + j\omega C/G_s}. \quad [1]$$

For the experiment, it is important to know the phase relation between incremental current changes resulting from small changes in the three circuit elements G, C, and G_s. The variations of Y with perturbations in the circuit elements are given by

$$\frac{\partial Y}{\partial C} = j\omega B^2(\omega) \quad [2]$$

$$\frac{\partial Y}{\partial G} = B^2(\omega) \quad [3]$$

$$\frac{\partial Y}{\partial G_s} = (G + j\omega C)^2 B^2(\omega)/G_s^2, \quad [4]$$

The publication costs of this article were defrayed in part by page charge payment. This article must therefore be hereby marked "*advertisement*" in accordance with 18 U. S. C. §1734 solely to indicate this fact.

Abbreviation: rms, root mean square.

* Present address: Laboratoire de Neurobiologie, Ecole Normale Supérieure, 46, rue d'Ulm, 75005 Paris, France.

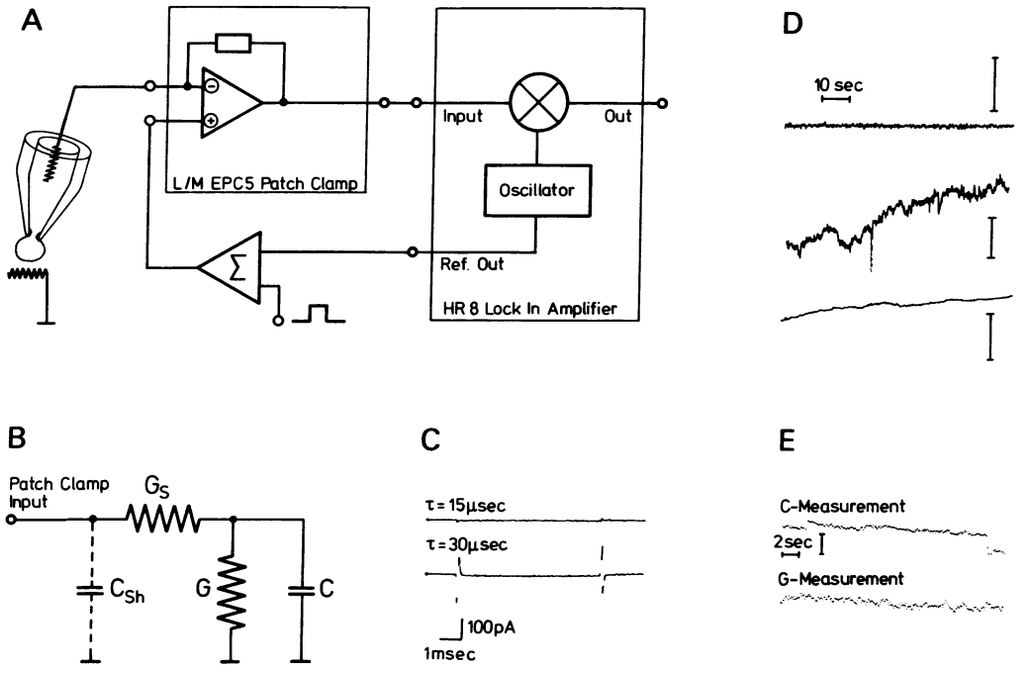

FIG. 1. Details of the capacitance measurement. (*A*) Block diagram of the instruments. A model HR8 lock-in amplifier (PAR, Princeton, NJ) is used in combination with an LM EPC-5 patch clamp (List Electronic, 61 Darmstadt 13, Federal Republic of Germany). The output of the lock-in amplifier is displayed both on the oscilloscope and on paper chart recorder (not shown). (*B*) Equivalent circuit for the pipette–cell assembly. The parallel combination of the cell G and C is assumed to be coupled to the amplifier input by a series conductance G_s (internal resistance of the pipette and of the pipette–cell connection). In addition, a shunt capacitance C_{sh} is indicated to represent stray capacitances mainly across the pipette wall. The patch-clamp circuit has provisions for compensating two components (a "fast" and a "slow" one) of capacitive current. (This is the capacitance transient cancellation network in the circuit of ref. 9). The fast component is used here to compensate C_{sh}. This adjustment is done immediately after gigaseal formation (9), before establishment of the whole-cell recording configuration. The required settings are stable at the fF level unless the pipette is moved or the fluid level is changed. Therefore, shunt capacitance is neglected in the analysis. (*C*) Capacitance cancellation. A model circuit with the values $1/G_s = 2\ M\Omega$, $1/G = 2\ G\Omega$, and $C = 4.7$ pF was used for these recordings. The upper trace shows a current response to a rectangular step of 9 mV in command potential (sinusoidal signal not applied here) after cancellation of capacitive current. The cancellation circuit (see ref. 9) was designed such that compensation involves simultaneous adjustment of two settings for the magnitude of the capacitance and for the time constant τ of the transient response, respectively. Optimal adjustment was obtained with $\tau = 15$ μsec (upper trace). Changing τ from 15 to 30 μsec led to a large inbalance (lower trace). An error of this magnitude corresponds to an error in α (with the numerical values given above) of 4°. The value of τ was measured several times during an experiment to prevent unnoticed drifts of α. The experiment was discontinued if τ increased above 60 μsec. (*D*) Background noise of the capacitance measurement. The top trace shows a paper chart record (5-Hz bandwidth) of the capacitance signal with the model circuit of C. Background noise in this record is 0.15 fF_{rms}. The middle trace shows a recording from a relatively silent cell—i.e., a cell with intracellular Ca^{2+} concentration buffered to 10 nM. Background noise is much higher than that of the model circuit, although the cell capacitance (5.3 pF) is very similar to that of the model circuit. The trace includes a truncated stimulus artifact. The bottom trace shows the noise in a "cell-attached" recording. Here, the background noise (≈0.1 fF_{rms}), apart from slow drifts, is smaller than in the model circuit. In all cases, a command signal of 18 mV_{rms} at 795 Hz (upper two traces) or 1,590 Hz (lowest trace) was used. (All calibration bars = 5 fF.) (*E*) Computer-aided recording at two orthogonal phase angles. The upper trace shows the signal recorded at a phase-setting ϕ appropriate for C measurement. This trace shows two characteristic steps. The lower trace shows the same signal at phase $\phi + 90°$. This signal should be proportional to membrane conductance. There is more noise associated with this signal. However, no discontinuities related to the above step changes are apparent. Vertical calibrations were 20 fF and 100 pS, respectively.

where $B(\omega) = 1/(1 + G/G_s + j\omega C/G_s)$. Eqs. 2 and 3 show that the argument ϕ of the response to small changes in C is orthogonal to that, α, of the signal resulting from membrane resistance changes. Eq. 4 shows that the error signal that might result from changes of G_s has an argument close to α because $\omega C \gg G$. Thus, for typical values of a chromaffin cell at rest, ($1/G = 2\ G\Omega$; $C = 5\ pF$) and for $\omega = 5 \times 10^3$, the argument of $\partial Y/\partial(G_s)$ coincides with α within approximately 2°. From these considerations, it is clear that capacitive changes can be well separated from fluctuations in G (e.g., the opening and closing of ionic channels) and from fluctuations in G_s (healing over of the ruptured membrane), provided the argument of the quantity $B^2(\omega)$ has been found. This was achieved by making use of the slow component of capacitance compensation of the patch-clamp circuit (see Fig. 1 legend), which was adjusted at the beginning of each measurement to completely cancel the cell capacitance currents. With proper adjustment, small changes of the capacitance compensation setting simulate changes of the cell membrane capacitance. We performed these changes (by hand) while looking for a phase setting (α or $\alpha + 180°$) on the lock-in amplifier where the resulting signal vanished. The desired phase ϕ for capacitance was then set orthogonal to α.

In some of our measurements, we used a PDP 11-34 laboratory computer, which was programmed in a way that, through its analog-to-digital converters and its digital-to-analog converters, it could operate like a lock-in amplifier. In addition, it determined the amplitude of a second signal component phase-shifted by 90° with respect to the chosen phase. This signal arises, then, from changes in conductance. These measurements were performed to confirm that the typical changes in signal to be described below occurred at the preset phase angle. No comparable signals were observed in the phase-shifted measurement (Fig. 1*E*).

In most experiments the "whole-cell" recording configuration of Hamill *et al.* (9) was used. Sine wave root-mean-square (rms) values of 5–20 mV and 800–1,600 Hz frequency were superimposed onto a holding potential close to −60 mV and onto

step commands, which were occasionally applied to stimulate secretion. In some cases, we made similar measurements in the "cell-attached" patch recording configuration (9). We used bovine chromaffin cells isolated as described (10) and kept in short-term (1–8 days) culture. For electrical measurements from the cells, "internal" media containing ATP were used, and Cl^- as the major anion was avoided (see Fig. 2 legend). Such media have been shown (6) to be particularly favorable for exocytosis in bovine chromaffin cells. Most experiments were carried out at room temperature.

Electron microscopy after glutaraldehyde fixation reveals three types of vesicles in adrenal chromaffin cells. Electron-dense granules with a diameter ranging from 0.1 to 0.4 μm (10, 11) contain the catecholamines packaged for exocytosis. Electron-lucent granules having a mean diameter of 0.08 μm (12) are thought to be formed after endocytosis. Finally, after extensive stimulation, large electron-lucent vacuoles 0.2–1 μm in diameter can be seen (6). Assuming spherical shape and a specific capacitance of 1 $\mu F/cm^2$, the expected capacitance values of the electron-dense granules and of the small and large electron-lucent vesicles are 0.3–5, $\approx$0.2, and 1–30 fF, respectively. For comparison, the background noise of capacitance recordings obtained with the above method corresponds to $\approx$0.1–0.5 fF at a bandwidth of 0–5 Hz (see Fig. 1*D*). Still better resolution can be obtained in the cell-attached recording configuration. Thus, if exocytosis of the largest chromaffin granules is a discrete event, the corresponding capacitance increase should be detectable. The capacitance decrease associated with the formation of a large vacuole, if it occurs through a discrete endocytotic event, should be even more prominent. Obviously, fusion and retrieval of many smaller granules may cause a noisy background.

RESULTS

The input capacitance *C* of the chromaffin cells studied ($\approx$10 μm in diameter) ranged between 2.5 and 6 pF. The calculated specific surface capacitance was close to 1 $\mu F/cm^2$ (13). We found that large variations of *C* (up to 50%) occurred in the course of an experiment (typically 30 min) depending on the intracellular medium. *C* was found to decline slowly if the pipette solution, which quickly equilibrated with the cell interior (13), contained a Ca^{2+}–EGTA buffer with high Ca^{2+}-binding capacity and low effective Ca^{2+} concentration (usually 11 mM EGTA/1 mM Ca^{2+} was used, corresponding at pH 7.2 to an effective free Ca^{2+} concentration, Ca_i^{2+}, of 10 nM). If the pipette solution contained a Ca^{2+}–EGTA buffer with Ca_i^{2+} $\approx$1 μM, *C* was found to increase. In many cells where the *C* increase was particularly marked, the cytoplasm took a granular appearance. In cells where a solution with low Ca^{2+}-buffering capacity was used (e.g., 0.1 mM EGTA with no Ca^{2+}), the changes were more variable; a slow capacitance increase (perhaps resulting from cell injury when establishing the pipette-cell connection) was often followed by an opposite trend at the end of the experiment. In several of the recordings shown, the slow changes appear as steady declines or increases of the *C* signal throughout the traces.

Superimposed on these slow trends, the *C* signal presented a noisy appearance. A typical rms value of this noise was 0.5–2 fF (bandwidth, 0.1–5 Hz) if the cell potential was held at a value of −60 mV. This background noise was particularly low if an internal solution of low Ca_i^{2+} and high Ca^{2+}-buffering capacity was used (Figs. 1*D* and 2, trace d). Occasionally, spontaneous *C* jumps showed up above the background noise (Fig. 2, trace c and below).

When the cell was depolarized above −20 mV, large changes of the cell conductance *G* were elicited, so that the value of α was altered. The signal from the lock-in amplifier could, then, not be considered as a *C* signal during the depolarization. However, it was possible to measure *C* shortly after the end of a potential jump because *G* returned to its resting value within 100 msec after such a stimulation. The results of such measurements are shown in Fig. 2.

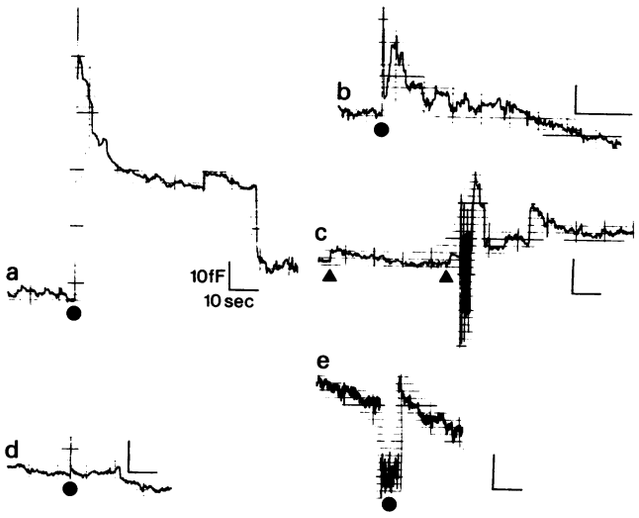

FIG. 2. Cell responses to depolarizing potential jumps. The bath solution was 140 mM NaCl/2.8 mM KCl/2 mM $MgCl_2$/1 mM $CaCl_2$ (except in trace e)/10 mM Hepes·NaOH, pH 7.2. The internal (pipette) solution contained 140 mM Na glutamate (traces a, b, and d) or K glutamate (traces c and e), 0.1 mM EGTA (except traces c and d), 2 mM $MgCl_2$, 5 mM ATP, and 10 mM Hepes·NaOH (or KOH) (pH 7.2). The holding potential was −67 mV in traces a, b, and d and −69 mV in c and e. (All calibration bars = 10 fF and 10 sec.) Traces a and b are typical responses with 0.1 mM EGTA in the pipette solution. In trace a, a 200-msec, 80-mV amplitude depolarization (●) elicited an 80-fF *C* increase, which was followed by a stepwise decrease. The 24-fF rapid decrease at the end of the record appeared on a faster time base to be due to several successive back-jumps. During the 80-mV depolarization, an inward cell current of 60 pA, carried by Ca ions, was observed. Thus, $\approx 3 \times 10^7$ Ca ions entered the cell during the depolarizing stimulus. In trace b, the responses to a 70-mV, 200-msec potential stimulation is shown (from another cell). The Ca^{2+}-current amplitude during the stimulus was 40 pA. Trace c shows the response in a cell with 1.5 mM EGTA/1 mM Ca^{2+} (calculated Ca_i^{2+}, 200 nM). ▲, Two spontaneous *C* jumps of 2–3 fF at the beginning of the record. After a 3.5-sec train of depolarizing pulses (10 Hz for 50 msec at 70 mV) a 20-fF *C* increase occurred, followed by stepwise *C* changes. Trace d shows the lack of response in a cell with 11 mM EGTA/1 mM Ca^{2+} (calculated Ca_i^{2+}, 10 nM) to an 80-mV, 200-msec voltage stimulation (●). Trace e shows the lack of response in a cell bathed in 1 mM Co^{2+} lacking Ca^{2+}. The internal solution contained 0.1 mM EGTA and no Ca (as in traces a and b). A 70-mV, 6-sec-long voltage pulse (●) failed to elicit a *C* signal. The change of the signal during the potential pulse and the stimulus artifacts of *c* are not necessarily related to actual changes of *C* for reasons explained in the text.

Marked effects were observed if the internal solution contained no Ca^{2+} and 0.1 mM EGTA (i.e., a low Ca_i^{2+} solution with low buffering capacity) (Fig. 2, traces a and b). The response consisted of a rapid capacitance increase followed by a slow return to the initial value. In many cases, the capacitance rise was too rapid to be resolved, or it occurred largely during the voltage pulse itself (Fig. 2, trace a). In other cases, a lag of a few seconds was observed before the maximum of the response, and indications of upward steps were obtained during this rise (Fig. 2, trace b). The shape of the capacitance decrease after the stimulation also varied greatly from cell to cell and from trial to trial. Occasionally, clear back steps were observed, but slow *C* decreases without obvious discontinuities were more common (Fig. 2, traces a–c). After large increases in *C*, very large back steps were often observed as late as 1 min after the voltage pulse (Fig. 2, trace a).

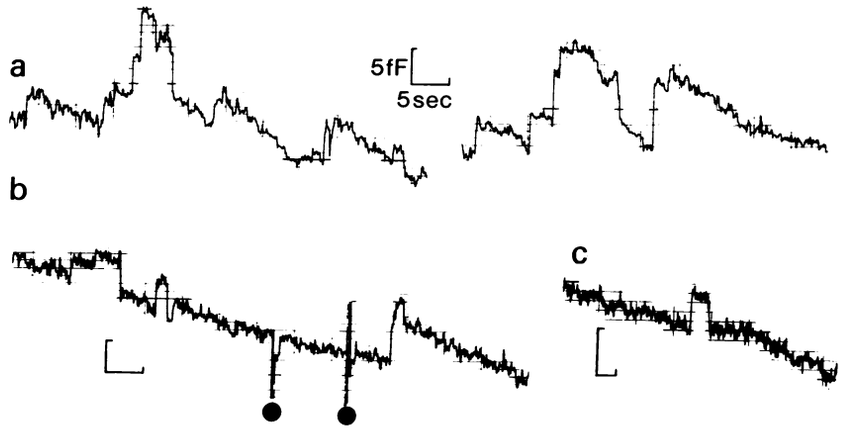

FIG. 3. On- and off-steps in whole-cell recordings. The pipette solutions were: 140 mM Na glutamate/2 mM $MgCl_2$/0.1 mM EGTA/10 mM Hepes·NaOH (trace a); 140 mM KCl/2 mM $MgCl_2$/1.5 mM EGTA/1 mM $CaCl_2$ (Ca_i, 200 nM)/10 mM Hepes·KOH (trace b); and 140 mM K glutamate/2 mM $MgCl_2$/1.5 mM EGTA/1 mM $CaCl_2$ (Ca_i, 200 nM)/5 mM ATP/10 mM Hepes·KOH (trace c). The membrane potential was −67 mV in trace a, −60 mV in trace b, and −69 mV in trace c. All three cells showed spontaneous on- and off-steps. The artifacts in trace b (●) correspond to two successive depolarizing voltage jumps of 60-mV amplitude lasting 20 and 200 msec, respectively. In trace c, an off-step follows an on-step of the same amplitude after 5 sec. (All calibration bars = 5 fF and 5 sec.)

When the Ca^{2+} concentration was buffered more strongly, the responses were smaller. In the example of Fig. 2, trace c, the pipette solution contained 1.5 mM EGTA/1 mM Ca^{2+} (calculated Ca_i^{2+} of 0.2 μM). The response amplitudes in Fig. 2, traces c and b are similar. However, a pulse train 3.5 sec long, with a total stimulus duration of 1.75 sec had to be applied for the response of Fig. 2, trace c, whereas a single pulse 200 msec long and of the same amplitude was sufficient in Fig. 2, trace b. If the pipette solution contained 11 mM EGTA/1 mM Ca^{2+} ($Ca_i^{2+} \approx 10$ nM), no *C* response could be elicited (three experiments; see Fig. 2, trace d).

The responses of Fig. 2 were presumably due to Ca^{2+} entry during the voltage pulse. This was indicated by the following lines of evidence. (*i*) The response was affected by the Ca^{2+}-buffering capacity of the cell. (*ii*) No stimulus-evoked response was observed if the external Ca^{2+} ions were replaced by Co^{2+} (Fig. 2, trace e). (*iii*) The responses could only be elicited for test potentials ranging between −10 and +40 mV. This is precisely the range where Ca^{2+} currents are large (14). In particular, pulses to +50 mV, as well as hyperpolarizing pulses, were ineffective.

The amplitude of the *C* response rapidly decreased if several identical voltage pulses were applied at short (1–5 sec) intervals. Also the *C* response slowly decreased with time, independently of stimulation, and no response was obtained 20–30 min after the start of the recording. This decline may be due to the "run-down" of Ca^{2+} currents which occurs in the same time range (14).

Spontaneous step-like capacitance increases (on-steps) and decreases (off-steps) were occasionally observed in the absence of voltage stimuli in cells with low-background noise. Examples of such steps are shown in Fig. 3. On- and off-steps were often better resolved at the end of an experiment, when the overall activity of a cell had decreased together with its sensitivity to voltage pulses. Both types of signal were present if the extracellular Ca^{2+} was replaced with Co^{2+}, or, if the intracellular

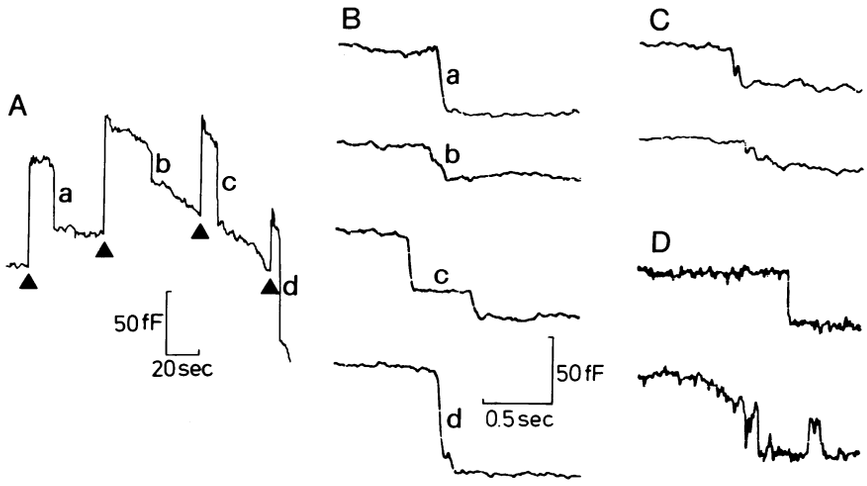

FIG. 4. Large amplitude off-steps in whole-cell recordings. (*A*) Low-speed recording from a cell bathed in normal saline and dialyzed with a K glutamate solution containing 0.1 mM EGTA (see legend to Fig. 2). The holding potential was −69 mV. Successive positive potential pulses of 500-msec duration and of 90-, 80-, 70-, and 60-mV amplitude elicited large *C* increases (▲), followed by four spontaneous off-steps (a, b, c, and d). (*B*) Same off-steps as in *A* displayed on a faster time scale. Only the first off-step (a) appeared as a single *C* jump, whereas the other off-steps were made of several (two in off-step c) successive jumps. (*C*) Two further examples of large spontaneous capacitance decreases with complex time courses (from the same cell). (*D*) Large spontaneous back-steps from another experiment performed under the same ionic conditions. Traces: upper, 40-fF single off-step; lower, capacitance decrease with a complex time course. Integration time constant of the lock-in amplifier: 30 msec (*B* and *C*) and 3 msec (*D*).

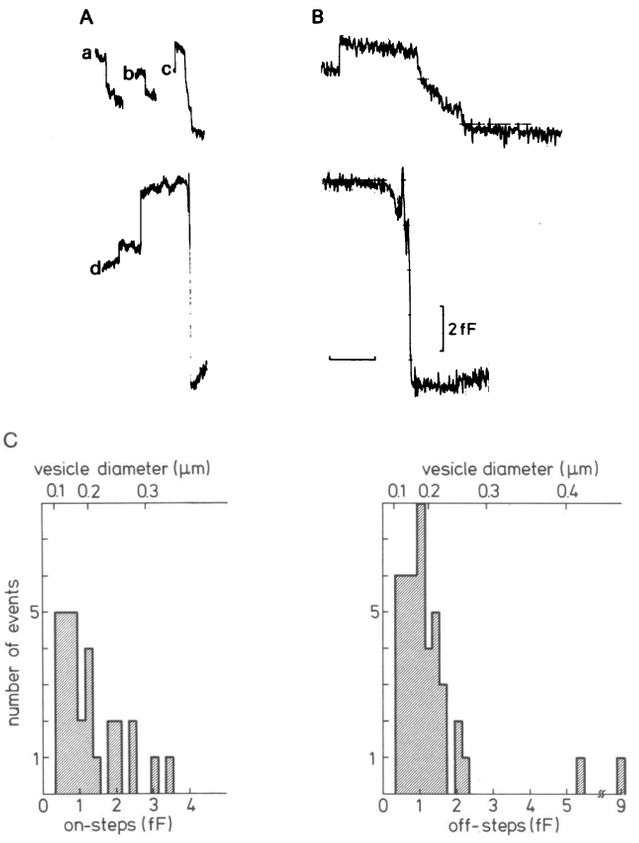

FIG. 5. On- and off-steps in a cell-attached recording. (*A*) Four successive recordings (traces a, b, c, and d) from a cell-attached patch. The pipette solution was normal saline with an increased Ca^{2+} concentration (5 mM). The pipette was held at the bath potential. Fast on- and off-steps may be seen in traces c to d and a to b, respectively. (*B*) The large *C* decrease of recording c in *A* (upper trace) and recording d in *A* (lower trace) are not due to single jumps. Horizontal calibration: 10 sec (*A*) and 2.5 sec (*B*). (*C*) Amplitude distribution of on- and off-steps. On- and off-steps were obtained in a total of 10 cell-attached patches. The pipette potential was the bath potential. One experiment was performed with a pipette solution of 1 mM Co^{2+} lacking Ca^{2+} (this patch displayed only off-steps); the other experiments were done with the same 5 mM Ca^{2+} as in *A* and *B*. Most results were obtained at room temperature, except for one patch where the measurements were made at 30°C. Both on- and off-steps had an average amplitude near 1 fF. The two off-steps larger than 5 fF (the largest of which is shown in *B*) had a complex time course, suggesting that they resulted from several smaller steps. (The *C* decrease shown in the upper trace *B* was not considered as an off-step and was rejected from the analysis). The upper scales indicate the calculated diameters of spherical vesicles corresponding to the capacitance values shown in the lower scales.

solution contained no ATP (Fig. 3, trace b), but they were not observed with 11 M EGTA/1 mM Ca^{2+} intracellular buffer. Off-steps were found to occur predominantly after on-steps. In rare cases, an off-step followed an on-step of the same size by 5–20 sec (Fig. 3, trace c). In most cases, however, the size of the off-steps did not appear to be related to that of the latest on-steps. In addition, many on- and off-steps occurred in isolation without obvious relation to events of the opposite polarity.

Large off-steps (20–80 fF) were typically observed after large or repeated *C* increases (Fig. 2, trace a). Their transition times were sometimes at least as fast as our time resolution (usually 30 msec), but, in the majority of the cases (as in Fig. 2, trace a), they appeared to be composed of successive off-steps. Sometimes on-steps also were interposed (Fig. 4).

Step-like changes in capacitance also could be observed in cell-attached recordings. Such recordings presented a lower background noise than whole-cell recordings so that steps as small as 0.4 fF could be resolved. The majority of patches failed to reveal any *C* steps, but others displayed as many as 20 on- and off-steps in a time span of roughly 10–20 min. Fig. 5 *A* and *B* shows examples of such steps and Fig. 5*C* shows the amplitude distribution of all on- and off-steps recorded with this method. Both on- and off-step amplitude distributions were maximal near 0.4 fF, the lowest step size that could be determined. This probably indicates that the true peaks of distribution occurred at values lower than 0.4 fF. The off-step amplitudes varied on a broader range than the on-step amplitudes. The largest off-steps consisted of several consecutive events (Fig. 5).

DISCUSSION

Our results demonstrate that the capacitance of the surface membrane of small cells such as chromaffin cells can be monitored at high resolution by the patch-clamp technique. Furthermore, we propose that the discrete changes in capacitance described above correspond to the fusion and to the retrieval of single vesicles. The evidence for that can be summarized as follows. (*i*) Off-steps were preferentially found after on-steps, as is expected from an exocytosis/endocytosis process. (*ii*) Spontaneous on- and off-steps were not recorded when Ca_i^{2+} was maintained at 10 nM but they were frequent when the Ca_i^{2+} level was more loosely controlled (0.1 mM EGTA solution) or when it was buffered at a higher level (0.2 μM). This is consistent with the dependence of catecholamine release on Ca_i^{2+} in chromaffin cells (6). (*iii*) The rate of occurrence of on- and off-steps could be greatly increased by giving depolarizing voltage pulses. This was attributed to Ca^{2+} entry during the depolarization. (*iv*) The amplitude distributions of on- and off-steps are in rough agreement with the distribution of the surface areas of chromaffin granules as determined from anatomical data when a unitary capacitance of 1 $\mu F/cm^2$ is assumed. (*v*) The observation of large vacuoles after stimulation (6) matches the present finding of large off-steps after large *C* increases.

We thank Dr. F. J. Sigworth for providing an assembler routine for our PDP 11/34 to perform the computer-aided measurements. A.M. was supported by the Centre National de la Recherche Scientifique.

1. Katz, B. (1969) *The Release of Neural Transmitter Substances* (Liverpool Univ. Press, Liverpool, England).
2. Trifaro, J. M. (1977) *Annu. Rev. Pharmacol. Toxicol.* **17**, 27–47.
3. Case, R. M. (1978) *Biol. Rev. Cambridge Philos. Soc.* **53**, 211–354.
4. De Robertis, E. D. P. & Sabatini, D. D. (1960) *Fed. Proc. Fed. Am. Soc. Exp. Biol.* **19**, Suppl. 5, 70–78.
5. Diner, O. (1967) *C. R. Hebd. Seances Acad. Sci. Paris* **265**, 616–619.
6. Baker, P. F. & Knight, D. E. (1981) *Phil. Trans. R. Soc. London B* **296**, 83–103.
7. Abrahams, S. J. & Holtzman, E. (1973) *J. Cell Biol.* **56**, 540–558.
8. Winkler, A. D. & Smith, H. (1972) in *Handbook of Experimental Pharmacology*, eds. Blaschko, H. & Muscholl, E. (Springer, Berlin), Vol. 33.
9. Hamill, O. P., Marty, A., Neher, E., Sakmann, B. & Sigworth, F. J. (1981) *Pflügers Arch.* **391**, 85–100.
10. Fenwick, E. M., Fajdiga, P. B., Howe, N. B. S. & Livett, B. G. (1978) *J. Cell Biol.* **76**, 12–30.
11. Unsicker, K., Griesser, G. H., Lindmar, R., Löffelholz, K. & Wolf, U. (1980) *Neuroscience* **5**, 1445–1460.
12. Benedeczky, I. & Smith, A. D. (1972) *Z. Zellforsch. Mikrosk. Anat.* **124**, 367–386.
13. Fenwick, E. M., Marty, A. & Neher, E. (1982) *J. Physiol. (London)* **331**, 577–597.
14. Fenwick, E. M., Marty, A. & Neher, E. (1982) *J. Physiol. (London)* **331**, 599–635.